THE JOURNAL OF PHYSICAL CHEMISTRY C

Article

pubs.acs.org/JPCC

The Nature of the Molybdenum Surface in Iron Molybdate. The Active Phase in Selective Methanol Oxidation

Catherine Brookes,[†,‡] Peter P. Wells,*[,†,§] Nikolaos Dimitratos,[†,§] Wilm Jones,[†,‡] Emma K. Gibson,[†,§] David J. Morgan,[‡] Giannantonio Cibin,[∥] Chris Nicklin,[∥] David Mora-Fonz,[§] David O. Scanlon,[§,∥] C. R. A. Catlow,[†,§] and Mike Bowker*[,†,‡]

[†]UK Catalysis Hub, Research Complex at Harwell Rutherford Appleton Laboratory, Harwell, Oxon, OX11 0FA, U.K.

[‡]Cardiff Catalysis Institute, School of Chemistry, Cardiff University, Main Building, Park Place, Cardiff, CF10 3AT, U.K.

[§]Kathleen Lonsdale Materials, Department of Chemistry, University College London, Gordon Street, London, WC1H 0AJ, U.K.

[∥]Diamond Light Source, Harwell Science and innovation Campus, Didcot, Oxon, OX11 0DE, U.K.

Supporting Information

ABSTRACT: The surface structure of iron molybdate is of great significance since this is the industrial catalyst for the direct selective oxidation of methanol to formaldehyde. There is a debate concerning whether $Fe_2(MoO_4)_3$ acts as a benign support for segregated MoO_3 or if there is an intrinsic property of the surface structure which facilitates its high catalytic efficacy. This study provides new insights into the structure of this catalyst, identifying a bound terminating layer of octahedral Mo units as the active and selective phase. Here we examine whether only 1 monolayer of Mo on iron oxide alone is efficacious for this reaction. For a 1 ML MoO_x shell−Fe_2O_3 core catalyst the Mo remains at the surface under all calcination procedures while exhibiting high selectivity and activity. The work highlights how catalyst surfaces are significantly different from bulk structures and this difference is crucial for catalyst performance.

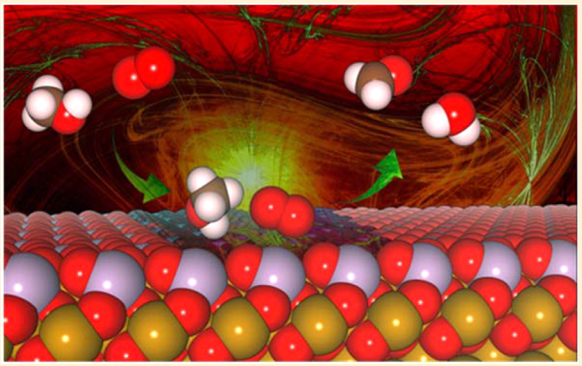

INTRODUCTION

The development of more efficient catalysts for industrial chemical processes is regarded as having significant economic benefits as well as having a positive impact on the wider society. To make step-change improvements in catalytic performance a fundamental understanding of the active site within catalytic systems is crucial. Iron molybdate is the primary catalyst for the selective oxidation of methanol to formaldehyde, which is of significant industrial importance, being used in production of resins and as a building block for higher value products. Commercial iron molybdate catalysts are typically formulated with an excess of Mo, since Mo is shown to volatilize from reactor hot spots during the reaction,[1,2] leaving an unselective Fe rich surface.[3] It is widely reported that this excess Mo segregates to the surface of these materials, as proven by STEM and EELS,[4] as well as HRTEM. However, this approach is shown to leave a system containing multiple distinct phases including both MoO_3 and $Fe_2(MoO_4)_3$, making it difficult to assess the nature of the active site. It is important to address whether $Fe_2(MoO_4)_3$ merely acts as a support for MoO_3 or whether it has its own inherent activity.[5−7] Bowker et al. have recently published work highlighting how bulk spectroscopic techniques such as XAFS (X-ray absorption fine structure) can yield crucial insights into the surface layers of core−shell mixed metal oxide catalysts.[8] The study involved the preparation of 3 monolayers (ML) of molybdenum deposited onto Fe_2O_3, followed by calcination at a range of temperatures (120−600 °C). The work demonstrated the presence of an octahedral (O_h) Mo oxide overlayer, even after extensive heating (600 °C, 2 h). This overlayer corresponds to one monolayer of the total molybdenum dosed, which was ascertained through XANES (X-ray absorption near edge structure) analysis. In view of this, it was proposed that the overlayer structure is the fundamental, active surface for the selective oxidation of methanol to formaldehyde, since catalysts prepared at varying calcination temperatures showed both similar activity and this structure in common. It is believed that this active layer is also directly related to iron molybdate catalysts used commercially. This paper addresses the question as to (i) whether one monolayer of the molybdenum oxide is sufficient to give a highly selective material and (ii) whether it all will remain at the surface of the material after high temperature annealing. In this instance where the Mo is present solely at the surface, conventional bulk characterization techniques such as XAFS can provide surface sensitive information.

Received: August 12, 2014
Revised: October 16, 2014
Published: October 16, 2014

   dx.doi.org/10.1021/jp5081753 | J. Phys. Chem. C 2014, 118, 26155−26161

EXPERIMENTAL SECTION

General Synthesis. A series of catalysts were prepared of MoO_x/Fe_2O_3 by doping 1, 3, or 6 monolayer equivalents of Mo oxide onto the surface of commercial Fe_2O_3 (Sigma-Aldrich, <50 nm particle size). The desired amount of aqueous ammonium heptamolybdate was dosed onto the surface of the Fe_2O_3 by incipient wetness impregnation. The samples were dried at 120 °C for 24 h, before being subjected to different annealing temperatures, in air, for 2 or 24 h.

Catalytic Testing. Reactor data was obtained by use of a CATLAB reactor (Hiden Ltd., Warrington, U.K.). For the catalytic reaction, 1 μL of liquid methanol was injected every 2 min into a flow of 10% O_2/He, at a flow rate of 30 mL min^{-1}. The products were determined by the online mass spectrometer in the CATLAB system. For the TPD, approximately 6 injections of 1 μL of methanol were dosed onto the catalyst, at ambient temperature in a flow of 30 mL min^{-1} of He. This was followed by ramping the temperature to 400 °C at a rate of 8 °C min^{-1}, while monitoring the products formed by mass spectrometry. Cracking patterns for different molecules were calibrated and were used in TPD selectivity determinations.

Characterization. The BET surface area was measured three times for each sample under nitrogen physisorption at 77 K using a Micromeretics Gemini surface area analyzer. Raman measurements were carried out using a Renishaw Raman microscope with an 830 nm laser power, over a wavenumber range of 100−1200 cm^{-1}. Typical measurements used a 0.1% laser power, with 4 accumulations at 10 s exposure time for each. XRD was performed on a Panalytical X'pert pro analyzer with Cu Kα radiation. The IR data were recorded using a Thermo Scientific Nicolet iS10 FT-IR spectrometer using an ATR accessory in the range of 500−2500 cm^{-1}.

Catalyst morphology and homogeneity were examined by TEM. The catalysts were examined using a JEOL JEM 2100 EM model and showed no obvious sign of particle clustering or agglomeration at the surface.

Mo k-edge XAFS studies were carried out on the B18 beamline at the Diamond Light Source, Didcot, U.K. Measurements were performed using a QEXAFS setup with a fast-scanning Si (111) double crystal monochromator. The time resolution of the spectra reported herein was 5 min/spectrum (k_{max} = 15); on average three scans were acquired to improve the signal-to-noise level of the data. All samples were measured in transmission mode using ion chamber detectors. All transmission XAFS spectra were acquired concurrently with a Mo foil placed between I_t and I_{ref}.

XAS data processing and EXAFS analysis were performed using IFEFFIT[9] with the Horae package[10] (Athena and Artemis). The amplitude reduction factor, S_0^2, was derived from EXAFS data analysis of known Mo reference compound, MoO_3 (with known coordination numbers which were fixed during analysis), to be 0.82, which was used as a fixed input parameter.

RESULTS AND DISCUSSION

The series of shell/core structures of MoO_x/Fe_2O_3 described herein were synthesized through incipient wetness impregnation of ammonium heptamolybdate[7,11] onto Fe_2O_3 (see Supporting Information for detailed description). By varying the concentration of ammonium heptamolybdate used, 1, 3, or 6 ML coverages of MoO_x were generated. The subsequent catalysts were calcined in air at holding temperatures of 300, 400, 500, and 600 °C for 2 h or 20 4 h to generate the active materials. The surface area of the catalysts was assessed using Brunauer−Emmett−Teller (BET) analysis, and there was no discernible loss in surface area after the different calcination regimes, with all MoO_x/Fe_2O_3 catalysts exhibiting approximately a 3-fold increase in surface area (15 m^2 g^{-1} to 5 m^2 g^{-1}, see Table S1 in the Supporting Information) compared to a conventional $Fe_2(MoO_4)_3$ catalyst. X-ray diffraction studies (XRD Figures S1 and S2 in the Supporting Information) were performed to identify any bulk phases produced. Additional phases beyond $\alpha - Fe_2O_3$ were only identified for the catalyst dosed with 6 monolayer equivalents of Mo, where separate phases of MoO_3 and $Fe_2(MoO_4)_3$ were identified at calcination temperatures of 300−500 °C and 500−600 °C, respectively. To verify that a core−shell structure is formed, TEM-EDX (transmission electron microscopy energy dispersive X-ray analysis) measurements were performed in order to provide information on nanoparticle morphology and spatial variation in elemental composition. Figure 1 is a TEM image for a particle of the 1 ML MoO_x/Fe_2O_3 catalyst calcined to 600 °C for 24 h. The associated TEM-EDX line profile, Figure 1, also illustrates the spatial composition of Mo, O, and Fe across a section of the particle. The Mo surface enrichment confirms the presence of a core−shell structure. This result was seen for different areas and particles, and for all three Mo coverages. Work by the groups of Routray and Bowker have also identified Mo segregation in bulk ferric molybdate catalysts using LEIS (low energy ion scattering),[7] and aberration-corrected STEM (scanning transmission electron mictroscopy) and EELS (electron energy loss spectroscopy) analysis, respectively.[4] Enrichment of Mo at the surface of these catalysts is also supported by XPS (X-ray photoelectron spectroscopy) (Figures S3 and S4 in the Supporting Information).

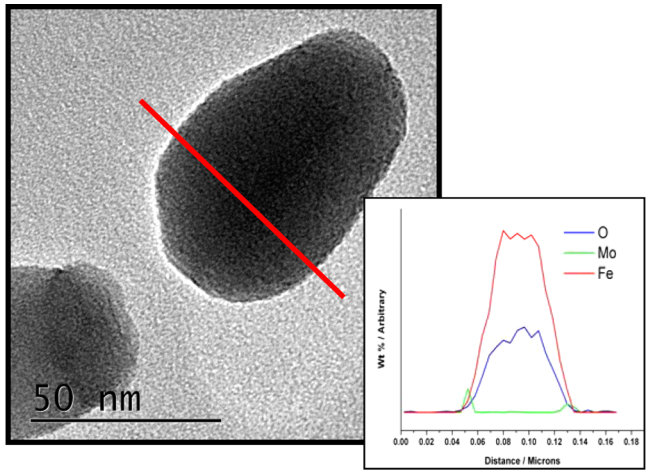

Figure 1. TEM micrograph of 1 ML MoO_x/Fe_2O_3 at 500 °C/24 h, with EDX line profile analysis. The elemental composition across the line is shown in the bottom right corner.

Mo k-edge XAFS measurements of the different MoO_x/Fe_2O_3 catalysts were performed to discern the extent of tetrahedral (T_d) and octahedral (O_h) character of the Mo sites, as well as provide information about the local environment. The interpretation of features in the Mo XANES spectra involves the assignment of the pre-edge peak at ~19995 eV and the peak at 20010 eV. The pre-edge peak is attributed to the

dx.doi.org/10.1021/jp5081753 | J. Phys. Chem. C 2014, 118, 26155−26161

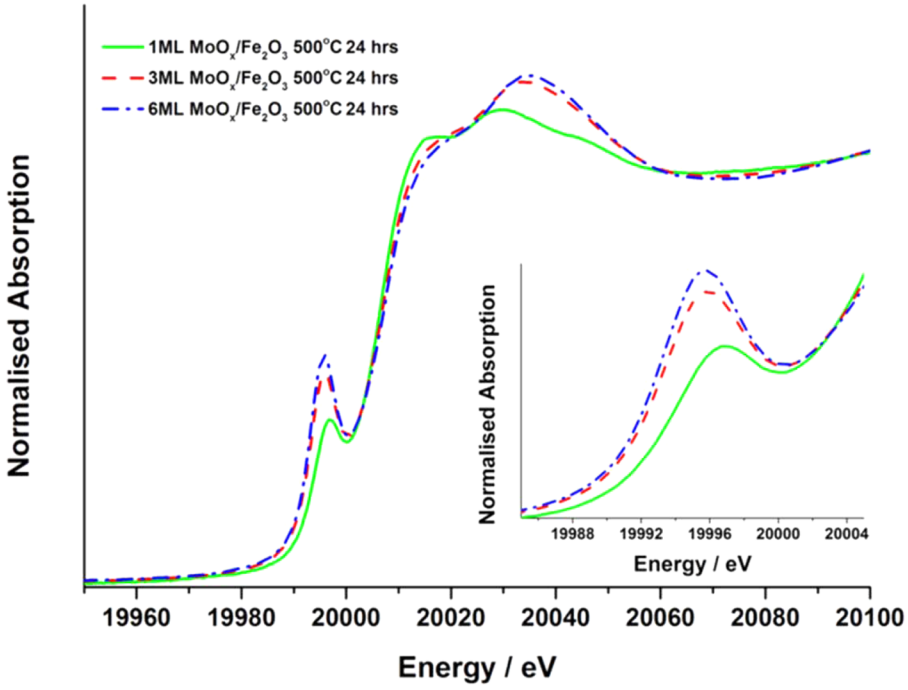

Figure 2. Normalized XANES data for the 1, 3, 6 ML catalysts calcined to 500 °C/24 h, with enlarged pre-edge region.

dipole forbidden/quadrupole allowed 1s−4d transition,[12] associated primarily with T_d geometry, but is also present, albeit weaker, in structures with distorted octahedral geometry.[13−15] The peak at 20010 eV is assigned to the dipole allowed 1s−5p transition and is a characteristic feature of Mo species with octahedral/distorted octahedral geometry.[13−15] The Mo k-edge XANES spectra for the three core−shell catalysts annealed at 500 °C for 24 h are presented in Figure 2 and show a greater degree of T_d character, indicative of the presence of iron molybdate, as the monolayer equivalent of Mo is increased.

For the catalyst in which there is just 1 ML equivalent of molybdenum, the catalyst is consistent with a distorted O_h geometry throughout the calcination range. It is therefore established that for monolayer (or sub-monolayer) amount of a species we label as MoO_x, the molybdenum remains segregated at the surface of the Fe_2O_3, with complete O_h geometry under all calcination conditions (Figure S5 in the Supporting Information). Indeed the same Mo XAFS spectrum was generated when a physical mixture of MoO_3 and Fe_2O_3 was exposed to the same calcination regime (as described in the Supporting Information). It is evident that this Mo surface is very stable, since it forms regardless of the preparation method employed. Table S2 in the Supporting Information gives the phase composition, obtained through linear combination fitting of the XANES data for these catalysts (Figure S6 in the Supporting Information). Results confirm that, with an increase in monolayer coverage, the O_h to T_d ratio varies, with the 6 ML catalyst exhibiting the greatest T_d character. Moreover, the phase composition generated by linear combination analysis of the XANES data confirms that all samples have approximately 1 ML of O_h Mo units present at the surface. If this trend is extended, it would be expected that even a bulk (stoichiometric) iron molybdate catalyst would have a surface terminating in O_h Mo units, and certainly enrichment of Mo in the surface region of such catalysts has been found.[1] Although XRD analysis was unable to identify any phases beyond $\alpha - Fe_2O_3$ for the 1 and 3 monolayer MoO_x/Fe_2O_3 catalysts, the phase composition generated by the XANES linear combination fits were supported by those assigned from vibrational spectroscopy (FT-IR and Raman) and are detailed in the Supporting Information (Figures S7−S15, Table S3).

EXAFS provides a valuable means of assessing the local structure of materials which do not possess long-range order. This is of importance for this work for identifying the nature of Mo at the surface. Figure 3 shows the non-phase-corrected Fourier transform of the k^2 weighted EXAFS data (plus imaginary components of the data and scattering paths) of the 1 ML MoO_x/Fe_2O_3 sample annealed at 500 °C for 24 h. The XANES data confirm the presence of O_h Mo units. The EXAFS shows that these units are bound to the Fe_2O_3 surface with a clear Mo−Fe interaction. The primary Mo O_h environment is composed of oxygen neighbors, with the major contribution at low values of R in the Fourier transform associated with a short Mo−O (distance = 1.74 Å) scattering path (Table 1). The longer Mo−O scattering path (distance = 1.95 Å) has less impact on the EXAFS data as a consequence of the large disorder associated with it. The combination of these two scattering paths results in a good correlation between the experimental and simulated data for values of R < 2 Å. The subsequent coordination environment (after 2 Å) is associated with the Mo−Fe scattering paths. Here the model used for the EXAFS fitting parameters was informed by the computational studies, described later, indicating a site where the Mo would have three Fe neighbors at around 3 Å and one Fe neighbor at a shorter distance. The relatively weak intensity of four Mo−Fe neighbors is a result of the out of phase behavior of the different Mo−Fe distances, as seen in the imaginary part of the Fourier transform (Figure 3).

Computational modeling was undertaken to determine the nature of the preferred adsorption site on the most stable surface (0001) of α-Fe_2O_3.[16] A neutral MoO_3 unit can be accommodated at five topologically distinct adsorption sites with mixed oxide−iron termination as shown in Figures 4 and

dx.doi.org/10.1021/jp5081753 | J. Phys. Chem. C 2014, 118, 26155−26161

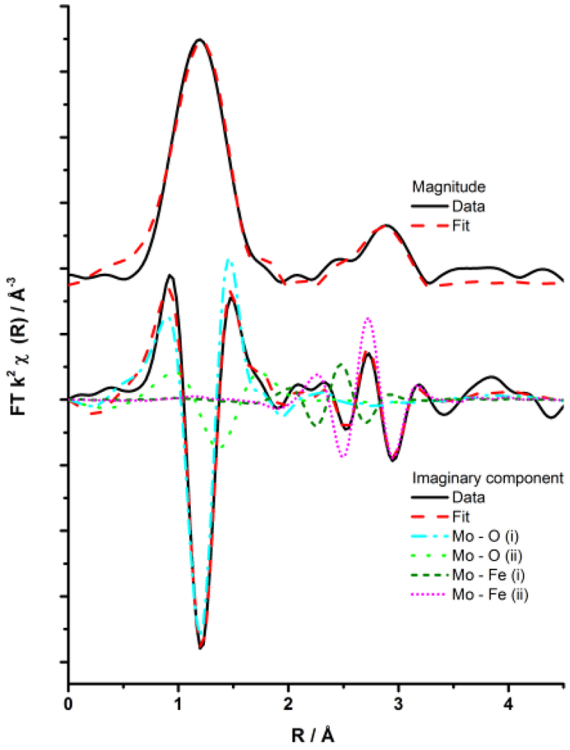

Figure 3. Magnitude and imaginary component of the k_2 weighted Fourier transform for the EXAFS data of the 1 ML MoO_x/Fe_2O_3 catalyst calcined to 500 °C/24 h. Associated scattering paths are included for the imaginary component.

Table 1. EXAFS Fitting Parameters for the 1 ML MoOx/Fe_2O_3 Catalyst Calcined to 500 °C[a]

abs sc	N	R/Å	$2\sigma^2$/Å^2	E_f/eV	R_{factor}
Mo−O	3 (fixed)	1.74(2)	0.006(1)	7(3)	0.005
Mo−O	3 (fixed)	1.95(6)	0.03(1)		
Mo−Fe	1 (fixed)	2.85(4)	0.009(6)		
Mo−Fe	3 (fixed)	3.10(3)	0.009(3)		

[a]Fitting parameters: S_0^2 = 0.82 as deduced by MoO_3 standard; fit range 2.6 < k <9.7, 1 < R <3.5; no. of independent points = 11.

5. To aid the characterization of the experimental site, a series of *ab initio*, DFT plane-wave calculations have been performed[16,17] (see Supporting Information) using (1 × 1) and (2 × 2) surface models with a MoO_3 neutral unit added to each of the candidate sites at ca. 3 Å away from the surface. On geometry relaxation it was observed that whenever the Mo was placed just above a surface oxygen (adsorption site D), it moved off this site and tended to stabilize above the Fe ion of the second (subsurface) layer adopting either configuration A or B (Figure 4).

With a surface interstitial site E as a starting point, the Mo relaxed slightly toward the surface as one of the molybdate O ions was displaced toward the first layer Fe forming a Mo−O−Fe bridge. The adsorption site C proved to be highly unfavorable: the Mo stayed above the uppermost Fe atom with no strong Mo relaxation; the neutral MoO_3 layer remained nearly flat at a nonbonding distance above the surface. At sites A and B, an especially large Mo relaxation into the surface was found, where it adopts an octahedral coordination: at the most stable site A, Mo has one neighbor Fe ion at 2.80 Å and three at 2.96 Å, whereas at site B it has three Fe neighbors at 2.94 Å and one at 3.05 Å. Adsorption site A agrees with the coordination numbers in the EXAFS analysis and shows a good agreement with most of the bond distances (Table S4 in the Supporting Information).

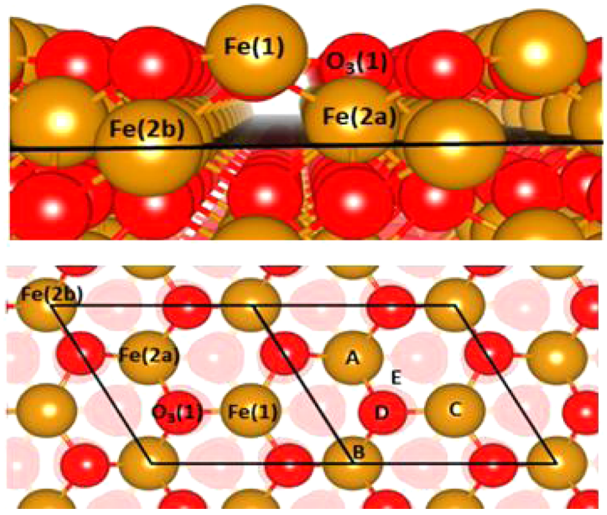

Figure 4. (Top) Side view of the α-Fe_2O_3 (0001) surface. The drawn plane marks the position of the semitransparent oxygen ions showed in the above picture. The brown and red spheres denote iron and oxygen respectively. (bottom) View along the hexagonal axis of the α-Fe_2O_3 (0001) surface. Different initial adsorption sites (from A to E) for the MoO_3 unit are shown; the rhombi represent the surface unit cell.

With a detailed understanding of the structural changes in the catalysts presented, it is important to relate these structural changes to catalytic performance, and for this purpose we used temperature-programmed desorption (TPD) of adsorbed methanol. Data obtained for the monolayer systems have been compared to reference standards, including MoO_3, Fe_2O_3, and $Fe_2(MoO_4)_3$. Results obtained are summarized in Figure 6 and further detailed in Table S5 and Figures S16−S21 in the Supporting Information. The TPD from the monolayer catalysts mainly yields formaldehyde, a product of absorbed surface methoxy. A slight amount of CO is also detected as the only byproduct of the reaction. There is no evidence of CO_2 production, which implies no extended Fe_2O_3 present at the catalyst surface. CO_2 is characteristic of Fe_2O_3, as a decomposition product from formate absorption (Figure S19 in the Supporting Information). Referring to Figure 6, it can be seen that the yield of formaldehyde improves with increasing monolayer coverage. For methanol oxidation, the 6 ML catalyst has a selectivity to formaldehyde of 87%, compared to that of the bulk $Fe_2(MoO_4)_3$ catalyst,[5] which demonstrates ~100% selectivity in TPD. The production of CO which contributes solely to this loss in selectivity, is proposed to derive from isolated Fe sites at the catalyst surface. It has previously been shown, through varying the Fe:Mo ratio in bulk catalysts, that an excess of Fe at the surface directly relates to the amount of CO produced. With Fe present, it is thought that the Mo−O−Fe bridging oxygen undergoes a change in binding energy to facilitate this extra dehydrogenation to CO. The presence of molybdenum dosed on the surface of the iron oxide clearly has a marked effect on the catalyst performance (Figures S18 and S19 in the Supporting Information). For Fe_2O_3, CO_2 is produced as the only significant product, with no evidence of formaldehyde. In comparison the 1 ML MoO_x/Fe_2O_3 shows no CO_2, with the selectivity to formaldehyde at 81% with the

dx.doi.org/10.1021/jp5081753 | J. Phys. Chem. C 2014, 118, 26155−26161

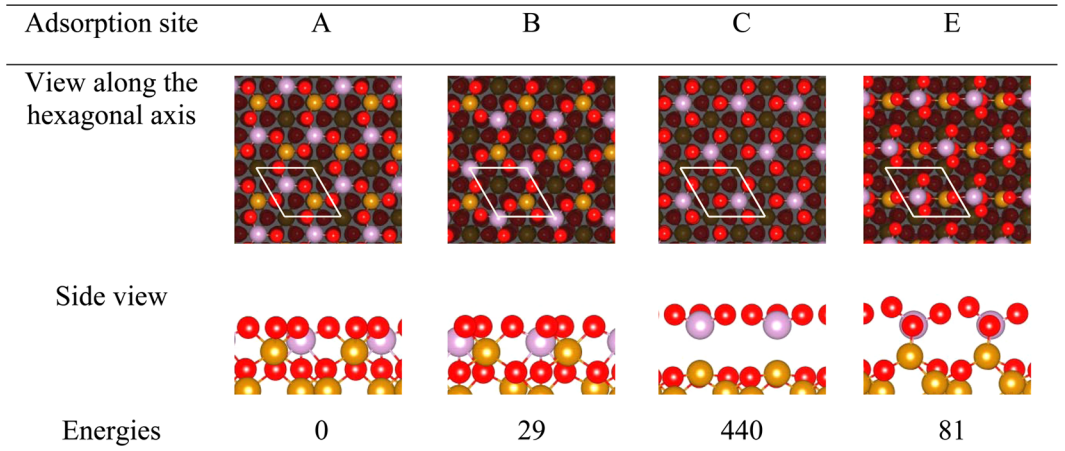

Figure 5. Relaxed structures for the different adsorption sites. Energies based on (1 × 1) surface calculation. The relaxed structure for the adsorption site D is not shown since it adopts either structure A or B. Red, brown, and violet spheres denote oxygen, iron, and molybdenum, respectively. Energies are in kJ mol^{-1}.

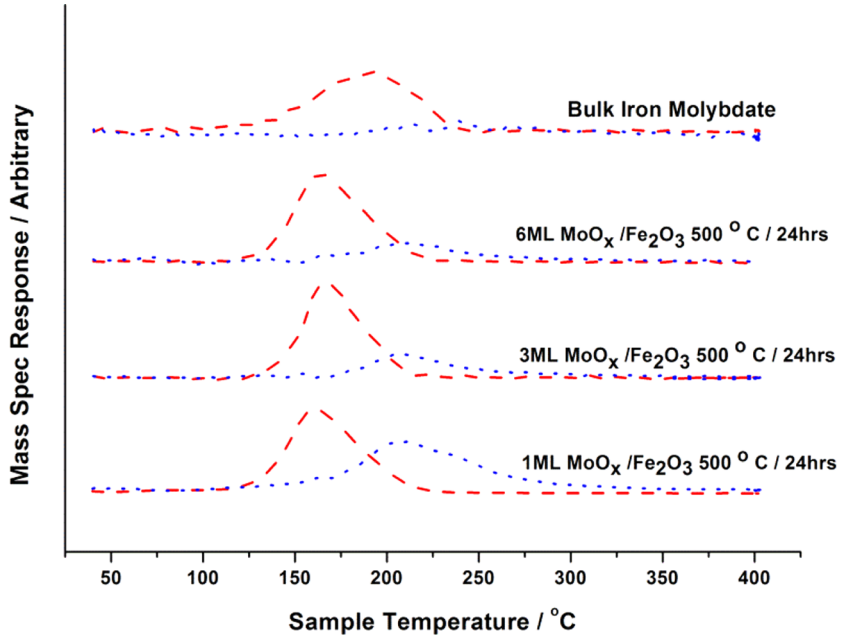

Figure 6. TPD data for bulk iron molybdate, compared with that of 1, 3, 6 ML MoO_x/Fe_2O_3 after calcining at 500 °C for 24 h. Mass: (red – – –) 30; (blue - - -) 28.

remaining 19% as CO. Although the data show lower selectivity than MoO_3 or $Fe_2(MoO_4)_3$, the catalyst shows a significantly improved activity with the temperature of H_2CO production at approximately 160 °C, as opposed to 191 and 205 °C for $Fe_2(MoO_4)_3$ and MoO_3, respectively (Table S5 and Figures S17, S20, and S21 in the Supporting Information). The amount of CO is believed to be controlled by the extent of the Mo coverage on the Fe_2O_3 surface. A corresponding study has investigated the effects of calcination length on catalyst performance (Figures S16 and S17 in the Supporting Information). It was found that, with increasing calcination time, the catalysts show a marked improvement in their selectivity, as a result of the Mo spread on the surface, and hence improvements in catalyst uniformity. Huang et al. have shown "spreading" of the MoO_3 phase over similar catalysts, demonstrating it to be a slow process requiring both harsh conditions and treatment times.[18]

Pulsed flow studies have been performed, in which methanol is pulsed over the catalyst every 2 min upon ramping the temperature of the catalyst bed to 400 °C at a ramp rate of 12 °C min^{-1}. These studies enable us to probe the catalyst's selectivity and conversion under more realistic reaction conditions. The MoO_x/Fe_2O_3 series of catalysts calcined at 600 °C for 24 h all exhibit a similar activity, which is superior to a conventional iron molybdate catalyst. This increase in activity is noticeable in the temperature for 50% conversion (T_{50}) values; 50% methanol conversion occurs at 190 °C for the 6 ML MoO_x/Fe_2O_3 (Figure S22 in the Supporting Information) a significant improvement over that for bulk $Fe_2(MoO_4)_3$, which only reaches the same conversion at 212 °C. It could be that this is due to the difference in surface area of these catalysts[19−21] (Table S1 in the Supporting Information). The MoO_x/Fe_2O_3 series of samples have a 3−4-fold increase in surface area compared to conventional iron molybdate catalysts, a benefit afforded by this preparation method. Despite slight

dx.doi.org/10.1021/jp5081753 | J. Phys. Chem. C 2014, 118, 26155−26161

changes in the onset of formaldehyde production, in general, all three monolayer loadings perform very similarly (Table S6 and Figures S22−S25 in the Supporting Information). This would agree with that already seen in the XANES, in which there is a common MoO_x phase present across the range of monolayer loadings. If future optimization can be made to improve the spread of this MoO_x and hence the selectivity further, this increase in surface area will lead to a much more efficient catalyst.

CONCLUSIONS

This study compares a series of $MoOx/Fe_2O_3$ catalysts to conventionally prepared $Fe_2(MoO_4)_3$ for the selective oxidation of methonal to formaldehyde. The catalyst screening studies shows that the performance of the two systems is comparable for all levels of Mo dosing on the MoO_x/Fe_2O_3 catalysts. Crucially, our investigations have shown that, for catalysts with a monolayer coverage of molybdenum on Fe_2O_3, an O_h overlayer of molybdenum oxide units remains at the surface and results in a very selective catalyst for methanol oxidation to formaldehyde. This layer is also present for multilayer catalysts and remains at the surface as the topmost and active layer. The implication of all these data is that a common active surface layer is present for all such catalysts, including bulk ferric molybdate catalysts of the type used industrially. Such materials can have higher surface area than the bulk molybdates, and so show potential for new catalysts for such processes. However, such potential can only be realized if selectivity is improved further and longevity of performance is properly demonstrated.

ASSOCIATED CONTENT

Supporting Information

The corresponding XRD, XPS, XAFS, BET, IR, Raman, and catalyst testing data. Further details on the modeling and experimental procedures carried out. This material is available free of charge via the Internet at http://pubs.acs.org.

AUTHOR INFORMATION

Corresponding Authors

*(M.B.) E-mail: bowkerm@cf.ac.uk.

*(P.W.) E-mail: peter.wells@rc-harwell.ac.uk.

Notes

The authors declare no competing financial interest.

ACKNOWLEDGMENTS

We acknowledge EPSRC for funding (EPI019693/1 and EP/K014714/1). Thanks also go to Diamond Light Source for provision of beamtime (SP8071-3) and for the contribution to the studentship of C. Brookes. The RCaH are also acknowledged for use of facilities and support of their staff. Via our membership of the U.K.'s HPC Materials Chemistry Consortium, which is funded by EPSRC (EP/L000202), this work made use of the facilities of HECToR and ARCHER, the U.K.'s national high-performance computing services, which are provided by UoE HPCx Ltd at the University of Edinburgh, Cray Inc and NAG Ltd, and funded by the Office of Science and Technology through EPSRC's High End Computing Programme. The work presented here made use of the High Performance Computing facility IRIDIS provided by the EPSRC funded Centre for Innovation (EP/K000144/1 and EP/K000136/1) which is owned and operated by the e-Infrastructure South Consortium formed by the universities of Bristol, Oxford, Southampton and UCL in partnership with STFC's Rutherford Appleton Laboratory. D.M.F. acknowledges support from CONACYT and UJAT Mexico. The authors thank Alexey A. Sokol for advice regarding the computational studies.

REFERENCES

(1) Ivanov, K. I.; Dimitrov, D. Y. Deactivation of an Industrial Iron-Molybdate Catalyst for Methanol Oxidation. *Catal. Today* **2010**, *154*, 250−255.

(2) Andersson, A.; Hernelind, M.; Augustsson, O. A Study of the Ageing and Deactivation Phenomena Occurring During Operation of an Iron Molybdate Catalyst in Formaldehyde Production. *Catal. Today* **2006**, *112*, 40−44.

(3) House, M. P.; Carley, A. F.; Bowker, M. Selective Oxidation of Methanol on Iron Molybdate Catalysts and the Effects of Surface Reduction. *J. Catal.* **2007**, *252*, 88−96.

(4) House, M. P.; Shannon, M. D.; Bowker, M. Surface Segregation in Iron Molybdate Catalysts. *Catal. Lett.* **2008**, *122*, 210−213.

(5) Soares, A. P. V.; Farinha Portela, M.; Kiennemann, A.; Hilaire, L.; Millet, J. M. M. Iron Molybdate Catalysts for Methanol to Formaldehyde Oxidation: Effects of Mo Excess on Catalytic Behaviour. *Appl. Catal., A* **2001**, *206*, 221−229.

(6) Soares, A. P. V.; Portela, M. F. Methanol Selective Oxidation to Formaldehyde over Iron-Molybdate Catalysts. *Catal. Rev. Sci. Eng.* **2005**, *47*, 125−174.

(7) Routray, K.; Zhou, W.; Kiely, C. J.; Grunert, W.; Wachs, I. E. Origin of the Synergistic Interaction between MoO_3 and Iron Molybdate for the Selective Oxidation of Methanol to Formaldehyde. *J. Catal.* **2010**, *275*, 84−98.

(8) Brookes, C.; Wells, P. P.; Dimitratos, N.; Cibin, G.; Morgan, D. J.; Jones, W.; Bowker, M. Molybdenum Oxide on Fe_2O_3 Core−Shell Catalysts: Probing the Nature of the Structural Motifs Responsible for Methanol Oxidation Catalysis. *ACS Catal.* **2014**, *4*, 243−250.

(9) Newville, M. IFEFFIT: Interactive XAFS Analysis and FEFF Fitting. *J. Synchrotron Radiat.* **2001**, *8*, 322−324.

(10) Ravel, B.; Newville, M. ATHENA, ARTEMIS, HEPHAESTUS: data analysis for X-ray absorption spectroscopy using IFEFFIT. *J. Synchrotron Radiat.* **2005**, *12*, 537−541.

(11) Bowker, M.; Brookes, C.; Carley, A. F.; House, M. P.; Kosif, M.; Sankar, G.; Wawata, I.; Wells, P. P.; Yaseneva, P. Evolution of Active Catalysts for the Selective Oxidative Dehydrogenation of Methanol on Fe_2O_3 Surface Doped with Mo Oxide. *Phys. Chem. Chem. Phys.* **2013**, *15*, 12056−12067.

(12) Ressler, T.; Timpe, O.; Neisius, T.; Find, J.; Mestl, G.; Dieterle, M.; Schlogl, R. Time-Resolved Xas Investigation of the Reduction/Oxidation of MoO_3-X. *J. Catal.* **2000**, *191*, 75−85.

(13) Beale, A. M.; Jacques, S. D. M.; Sacaliuc-Parvalescu, E.; O'Brien, M. G.; Barnes, P.; Weckhuysen, B. M. An Iron Molybdate Catalyst for Methanol to Formaldehyde Conversion Prepared by a Hydrothermal Method and Its Characterization. *Appl. Catal., A* **2009**, *363*, 143−152.

(14) Massa, M.; Haggblad, R.; Hansen, S.; Andersson, A. Oxidation of Methanol to Formaldehyde on Cation Vacant Fe-V-Mo-Oxide. *Appl. Catal., A* **2011**, *408*, 63−72.

(15) Radhakrishnan, R.; Reed, C.; Oyama, S. T.; Seman, M.; Kondo, J. N.; Domen, K.; Ohminami, Y.; Asakura, K. Variability in the Structure of Supported MoO_3 Catalysts: Studies Using Raman and X-Ray Absorption Spectroscopy with Ab Initio Calculations. *J. Phys. Chem. B* **2001**, *105*, 8519−8530.

(16) Rohrbach, A.; Hafner, J.; Kresse, G. *Ab Initio* Study of the (0001) Surfaces of Hematite and Chromia: Influence of Strong Electronic Correlations. *Phys. Rev. B* **2004**, *70*, 125426.

(17) Kresse, G.; Hafner, J. *Ab Initio* Molecular-Dynamics Simulation of the Liquid-Metal−Amorphous-Semiconductor Transition in Germanium. *Phys. Rev. B* **1994**, *49*, 14251−14269.

(18) Huang, Y.; Cong, L. Y.; Yu, J.; Eloy, P.; Ruiz, P. The Surface Evolution of a Catalyst Jointly Influenced by Thermal Spreading and

Solid-State Reaction: A Case Study with an Fe_2O_3-MoO_3 System. *J. Mol. Catal. A: Chem.* **2009**, *302*, 48−53.
(19) Arruano, J.; Wanke, S. Effect of High Temperature Treatment on the Properties of Fe/Mo Oxide Catalysts. *Can. J. Chem. Eng.* **1975**, *53*, 301−307.
(20) Soares, A. P. V.; Portela, M. F.; Kinnemann, A. Methanol Selective Oxidation to Formaldehyde over Iron-Molybdate Catalysts. *Catal. Rev.* **2005**, *47*, 125−174.
(21) Trifirò, F.; Notarbartolo, S.; Pasquon, I. The Nature of the Active Component in a Fe_2O_3-MoO_3 Catalyst. II. Study of the Variations Occurring During High Temperature Treatment. *J. Catal.* **1971**, *22*, 324−332.